The evolution characteristics of water absorption, hydration products and microstructure of supersulfated cement containing phosphogypsum by microbial induced carbonate precipitation

Lu Wang[a], Xiao Liang[a], Zhisheng Ren[a], Fuhao Gao[a], Shuhua Liu[a,*], Mingzhong Zhang[b]

[a] State Key Laboratory of Water Resources Engineering and Management, Wuhan University, Wuhan, Hubei, 430072, P.R. China

[b] Department of Civil, Environmental and Geomatic Engineering, University College London, London, WC1E 6BT, UK

[*]Corresponding author: shliu@whu.edu.cn

Abstract:

In this paper, microbial induced calcite precipitation (MICP) was adopted as a modifying technology for surface property enhancement of supersulfated cement (SSC) containing phosphogypsum (PG). A series of tests including waster absorption test, mercury intrusion porosimetry (MIP), X-ray diffractometry (XRD), thermogravimetric analysis (TGA) and scanning electron microscopy (SEM) were conducted to investigate the modification mechanism of SSC containing PG. The results indicate that the enhancement of surface properties is highly dependent on the modification methods and conditions. The effect of surface treatments on the reduction of water absorption and the refine of pore structure is superior to that of the direct-addition method (DM). After surface treatment, the content of ettringite slightly drops, while the calcite content rises significantly. TM with the volume ratio of bacterial solution to cementation solution of 1:1 leads to the formation of more bio calcite with spherical or square particles, which can fill the inner pores and surface holes of the surface layer. The increase of treatment cycle has a limited effect on the increase of calcite content, while can refine the pore structure and reduce the absorption coefficient when the treatment cycle was 9. DM has a great influence on the alkalinity of SSC mortar, which can significantly reduce the content of ettringite and slightly increase the calcite content and it also changes the morphology of ettringite in matrix.

Keywords: Supersulfated cement; Microbial induced calcite precipitation; Surface property; Pore structure; Morphology.

1. Introduction

Portland cement is the dominant binder in concrete for civil infrastructures not only due to its superior mechanical properties, high durability, but also for its low production cost and easy to cast into different shapes [1]. However, the production of Portland cement is an energy-intensive and resource-intensive process, resulting in approximately 0.87 tonne of CO_2 emission for every tonne of cement produced [2], inducing an increasing pressure to achieve sustainable development. Thus, it is vital to find alternative binders with lower CO_2 emissions and lower consumption [3, 4], while it is still a big challenge for the cement industry to achieve this target [5].

Supersulfated cement (SSC) composed of large amount of industrial by-products [6, 7] and less clinker, is a type of eco-friendly and energy-saving cement different from ordinary Portland cement [8]. Among the industrial by-products, ground granulated blast-furnace slag (GGBS) is the main raw material (accounting for 75-85% by mass) for preparing SSC, which is a glassy and granular material using water quenching molten blast furnace slag and it has latent hydration activity [9, 10]. SSC needs some sulphate activator with 10-20% content and alkaline activator with 0-5% content to active the hydration of GGBS [11, 12]. Dihydrate gypsum and anhydrite are always used as sulphate activators to produce SSC, which would increase the cost of SSC production. Phosphogypsum (PG) is an industrial by-product produced from wet phosphoric acid production and the main composition of which is dehydrate gypsum, as well as few F, P or other impurity matters [7, 13-16]. The accumulation of PG is more than 400 million tons, which not only occupies large of amount of land but also cause pollution to the surrounding environment. PG has been studied to prepare SSC, while it can prolong the setting time and induction period to some extent due to the impurity matters [17, 18], which restricted the use of PG in SSC. Calcination is a good pre-treatment method, which has been taken to remove the impurity matters to improve the property of SSC containing PG, such as faster setting time, higher compressive strength and denser pore structure [7, 19]. After the calcination of PG, the soluble phosphorus can be turned into calcium pyrophosphate (CaP_2O_7), which is water insoluble and harmless [19, 20] and thus can be used to shorten the setting time of SSC without reducing its mechanical strengths [13, 19]. The compressive strength of SSC containing calcination PG was significantly improved [19], along with good resistance to sodium sulphate attack [21]. In addition, SSC containing PG has the potential to reduce CO_2 emission compared to ordinary Portland cement [22-24], as it mainly consists of GGBS, PG and less clinker with specific surface area of 300-450 m^2/g. Therefore, SSC containing PG is considered as a promising low-carbon alternative binder to ordinary Portland cement for concrete.

Microbial induced calcite precipitation (MICP) is an attractive technology with ecological friendliness [25, 26], which has been widely adopted for surface protection of cement-based materials [27-30]. During the process of MICP, urea is decomposed into ammonium and carbonate by urease

produced by urease-bacteria, leading to a rise in pH and carbonate concentration. With the presence of Ca^{2+}, the precipitation of calcium carbonate occurs if the system is oversaturated. Once it happens on the surface of cement-based materials, a layer of calcite can be deposited on the surface, resulting in a drop in capillary water uptake and permeability [25, 30]. SSC concrete structure in service would suffer from atmospheric moisture, and which would lead to lower surface property [1, 31] and hinder its widespread application.

Meanwhile, the pH of pore solution in SSC paste was found to be about 11.5, which is lower than that in ordinary Portland cement system. Thus, low alkalinity SSC may provide a proper environment for the survival of urease-bacteria [32]. Combination between SSC and MICP may increase the properties of SSC from macro performance to microstructure. Otherwise, MICP has been proved to be acted as surface repair agent in OPC, it can also act on the surface or the internal in SSC to increase the property of the surface layer or the whole property by altering the hydration products and pore structure, and thus would be an effective method to improve the surface property of SSC.

The main purpose of this study is to systematically investigate the evolution characteristics of water absorption, hydration products and microstructure of SSC containing PG by MICP at different treatment methods and conditions, revealing the microscopic features that affect macroscopic properties of SSC mortar. Water absorption test was conducted to measure the absorption property of the surface including capillary water absorption coefficient and water absorption, hydration products were tested by X-ray diffractometry (XRD), thermogravimetric analysis (TGA), while the microstructural features were characterised using mercury intrusion porosimetry (MIP), and scanning electron microscopy (SEM). Firstly, the macroscopic properties of the surface of SSC mortar were measured. Afterwards, a series of statistical analysis were performed to explore the evolution of micromechanical properties of SSC mortar at different methods and conditions. Finally, the modification efficiency of MICP was discussed in detail from the viewpoints of conditions and treatment methods.

2. Experimental program

2.1. Raw materials

In this study, SSC composed of 80% GGBS, 15% calcination phosphogypsum (PG) and 5% Portland cement clinker (PCC) was produced with surface area of 380 m^2/kg. GGBS was supplied by Shanghai Baotian New Building Materials Co., Ltd., while PG was provided by Wuhan Zhongdong Phosphate Technology Co., Ltd. which was calcined at 350 ºC with calcination time of 2 h and could accelerate the setting obviously and enhance the workability [19]. PCC was obtained from Huaxin Cement Co., Ltd. The chemical compositions of these raw materials are listed in **Table 1**. Standard river sand as per GSB 08-1337-2018 was used as fine aggregate to prepare SSC mortar.

The bacterial solution (BS) used was stable bacterial solution, which was cultured in laboratory

and the details of the cultivation can be found in previous studies [33, 34]. The absorbance at the wave of 600 nm of BS was about 1-1.2, and its urease activity was about 30-35 mM urea/min. Chemical reagents containing calcium chloride (CC) and urea with the degree of AR grade were purchased from China National Pharmaceutical Group Corporation, which can be prepared for cementation solution (CS) with the concentration of 1 mol/L, and the mole ratio of CC and urea was 1:1.

Table 1 Chemical compositions of raw materials (wt.%).

Materials	CaO	SO_3	SiO_2	P_2O_5	Al_2O_3	Fe_2O_3	MgO	Na_2O	K_2O	TiO_2	F	Cl	CO_2	Others
GGBS	41.57	2.38	29.24	0	14.36	0.58	7.98	0.45	0.29	1.45	0	0.05	1.06	0.59
PG	24.01	33.93	7.84	2.47	1.37	1.21	0.33	0.1	1.25	0	5.03	0	22.13	0.33
PCC	63.49	1.77	20.23	0.15	5.35	3.72	1.22	0.5	0.79	0	0	0.04	1.98	0.76

2.2. Mix proportions and specimen preparation

SSC mortar specimens with the size of 40 mm × 40 mm × 40 mm, water to cement ratio of 0.5 and cement to sand ratio of 1:3 were mixed and casted under an ambient condition (20 ± 2 °C, ≥ 50% RH) and cured in a standard curing room (20 ± 1 °C, ≥ 90% RH) after de-moulding at 2 d. When the curing age was reached to 28 d, SSC mortars were put into a drying oven with 45 °C for 2 h to remove the water mark on the surface. For each specimen of surface treatment methods (top-surface-impregnation method and lower-surface-immersion method), one surface was selected as the treated face for capillary water absorption test, while the surrounding four surfaces were sealed with epoxy resin and aluminium adhesive to ensure unidirectional absorption. The whole procedure can be referred to Ref. [30]. No treatment was done for the specimen with direct-addition method.

The three methods adopted include: (1) Top-surface-impregnation method (hereinafter referred to as TM), which relied on natural deposition by gravity and the details can be found in Ref. [30]. (2) Lower-surface-immersion method (hereinafter referred to as LM), which relied on resorption deposition: after 28 d of curing, one cycle of the lower-surface-immersion process was employed on the specimens, as illustrated in **Fig. 1**. The test surface was soaked with 5 mm depth in bacterial solution with continuous stirring by magnetons for 12 h, and then taken out and soaked in cementation solution for another 12 h with soaking depth of 1 cm. The one cycle treatment lasted 1 d, and the treated numbers were set as 3, 6, 9 and 12 times. After the treatment, the specimen was put in an oven with 30 °C for 48 h. (3) Direct-addition method (hereinafter referred to as DM): given that the SSC system has a low pH of ~11.5, to investigate the effect of bacterial solution on the properties of SSC mortar, different proportions of bacterial solution of 0, 10%, 30% and 50% were employed to replace water in SSC mortar; during the curing, cementation solution with 10 mL was sprayed on six surfaces of all samples every day until the age of 28 d.

Considering the three different MICP methods above, the mix proportions of SSC mortar cubes adopted in this study including the parameters related to MICP methods are displayed in **Table 2**.

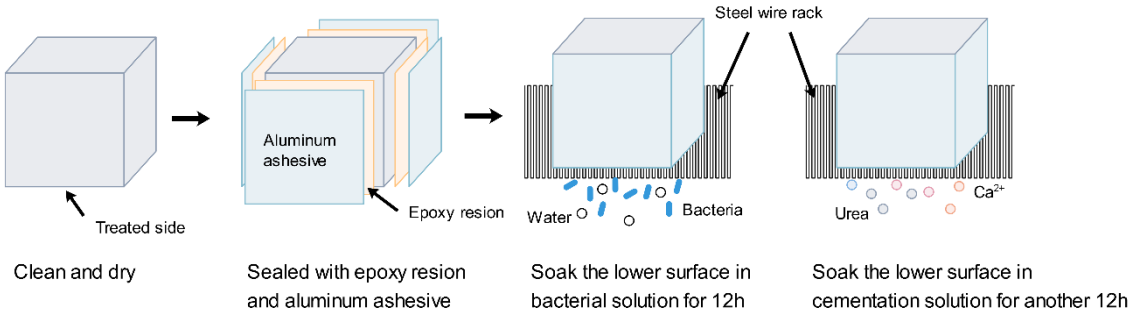

Fig. 1. Schematic illustration of the procedure of lower-surface-immersion method with MICP.

Table 2 Mix proportions of SSC mortar cubes and the parameters of MICP adopted in this study.

Samples	Mortar mix (g)			Important parameters related to different MICP methods			
	SSC	Sand	Water	Treated method	Bacterial solution	Cementation solution	Treated time
T-0	450	1350	225	Top-surface-impregnation	-	-	No treated
T-05					6 mL	12 mL	24 h
T-10					9 mL	9 mL	24 h
L-0	450	1350	225	Lower-surface-immersion	-	-	No treated
L-03					Sufficient content	Sufficient content	3 cycles
L-06							6 cycles
L-09							9 cycles
L-12							12 cycles
D-0	450	1350	225	Direct-addition	-	-	Standard curing for 28 d
D-10					10%	10 mL /d, spraying on six surfaces	28 d
D-30					30%		
D-50					50%		

2.3. Test methods

2.3.1 Water absorption test

After treated with TM, the extra aluminium adhesive on the treated surface was peeled off. All treated samples with TM and LM were dried in an air drying oven with the temperature of 60 °C until the difference in the mass loss ratio within 24 h was below 0.1%, and the ultimate mass was recorded as the initial weight. Then put the treated surface in water with the depth of 10±1 mm and weighted after drying with a wet towel [26] at designed time intervals (i.e., 0.5, 1, 2, 4, 8, 12, 24, 36 and 72 h). After the test, the capillary water absorption coefficient can be calculated based on the above data. More details of this test can be found in Ref. [30].

After treated by DM curing for 28 d, the water absorption dynamic test was carried out on SSC mortar specimens to evaluate the influence of bacterial solution on the properties of SSC mortar, following a procedure: 1) clean up the surface of SSC mortar and put it into an oven with the temperature of 105 ºC until the constant weight was reached, and then measure the dry weight m_0; 2)

put SSC mortar in water for 0.25 h, and measure the weight in the air as $m_{0.25}$ and the weight in water as $m_{0.25}^{w}$; 3) put SSC mortar in water till 1 h and then measure the weight in the air as $m_{1.0}$ and the weight in water as $m_{1.0}^{w}$; 4) put SSC mortar in water till 24 h, and then measure the weight in the air as m_{24} and the weight in water as m_{24}^{w}. Based on these data collected, the absorption (W_G), pore uniformity coefficient (α) and the average pore size (λ) can be calculated as follows:

$$W_G = \frac{m_{24} - m_0}{m_0} \cdot 100\% \tag{1}$$

$$\alpha = \ln\left[\ln\left(1 - \frac{W_{t2}}{W_{max}}\right) \Big/ \ln\left(1 - \frac{W_{t1}}{W_{max}}\right)\right] / \ln\left(\frac{t_2}{t_1}\right) \tag{2}$$

$$\lambda = \ln\left(\frac{W_{max}}{W_{max} - W_t}\right) \cdot t^{\alpha} \tag{3}$$

2.3.2 Mercury intrusion porosimetry (MIP)

Pore structure of the broken debris close to the treated surface (about less than 10 mm) of samples treated by TM and LM, the interior substance of samples treated by DM were characterised using MIP with the type of AutoPore Iv 9510 produced by American Mike Pretic.

2.3.3 X-ray Diffractometry (XRD)

The surface layers of specimens with surface treatment methods (TM and LM) and the interior substances of specimens with DM were collected to preserve in anhydrous ethanol to stop further hydration. And then some preserved samples were picked up to grind till the grinding powder without sense of particles to characterise the compositions and contents of hydration products. XRD was tested by X-ray diffractometry produced by RIGAKU, with copper target and continuous scan of 10º - 60º, step size of 0.02º and scanning rate of 5 º/min.

2.3.4 Thermogravimetric analysis (TGA)

The TGA spectra recorded at a thermal analysis equipment TGA2 produced by Mettler-Toledo, Switzerland, were monitored in the temperature range of room temperature (~30 ºC) to 1000 °C with a heating speed of 10 ºC/min and under a 30 ml/min flow of N_2 atmosphere. The weight loss of a specimen was used to calculate the phase contents of SSC mortar, including ettringite, C-S-H, and bio calcium carbonate.

2.3.5 Scanning electron microscopy (SEM)

The surface layers and interior substances of specimens with TM and LM, and only interior substances of specimens with DM were picked out to conduct SEM test to analyse the surface morphology and accumulation state of calcium carbonate particles deposited on the surface. The equipment used was field emission scanning electron microscope (Zeiss SIGMA) with accelerating voltage of 5 kV. The magnification was 5× - 100,000× and the resolution was 1.0-2.0 nm.

3. Experimental results

3.1. Macroscopic property water absorption

3.1.1. Capillary water absorption coefficient

Fig. 2 presents the capillary water absorption coefficients of SSC specimens after MICP treatment using the methods of TM and LM, indicating that SSC mortar treated by MICP exhibited a reduced water absorption coefficient. Specimens with TM showed a high drop in absorption coefficient which was about 67% and 71% of that of the specimens treated with B:S ratios of 1:2 and 1:1. The absorption coefficient of the specimen with B:S of 1:1 was 0.38 kg/($m^2 \cdot h^{1/2}$), whose reduction was higher than that of the specimen with B:S of 1:2 with the absorption coefficient of 0.43 kg/($m^2 \cdot h^{1/2}$), which can be attributed to the precipitation property of the formed bio calcium carbonate. The absorption coefficients obtained in this experiment are similar to that result of 399g/($m^2 \cdot h^{1/2}$) acquired by spraying method, which was provide more bacterial solution and CS[35]. For B:S = 1:1, the content of the precipitated bio calcium carbonate was higher [30, 34]. The more the bio calcium carbonate grains formed on the surface layer, the more the grains could fill in the pores. Moreover, the density of the surface layer increased and the filling effect of pore by bio calcium carbonate grains was better. For SSC specimens with LM, the water absorption coefficients dropped with the increase of treated numbers and the reduction were 35%, 48%, 63% and 62% of the samples treated for 3, 6, 9 and 12 times, respectively. There was a reduction tendency of the absorption coefficient when the treated number was up to 9 times, while the coefficient changed little when the treated number went up from 9 to 12 times. The reduction in absorption coefficient for specimens with LM can be explained by the fact that when the lower-surface of the sample was immersed in bacterial solution, some bacteria can be absorbed on the surface or permeate through the pores of the surface layer due to the movement of bacterial solution, and the bacterial metabolism near the surface layer can generate urease, which can decompose urea and form carbonate to absorb calcium ions in the system, resulting the in-situ precipitation of calcium carbonate to further fill the near surface pores. With the increase of treated numbers, the pores in the surface layer were filled gradually and accordingly the absorption coefficient dropped gradually. When the treated time was 9, the sediment on the surface was more, which filled in the large parts of the pores and more treated times had no effect on the density of surface layer.

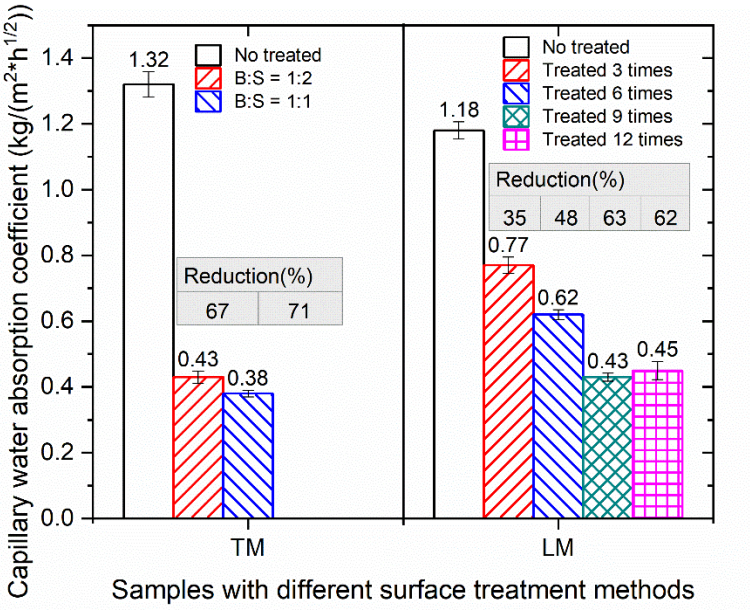

Fig. 2. Capillary water absorption coefficients of specimens with different surface treatments (B:S represents the volume ratio of bacterial solution to cementation solution).

3.1.2. Water absorption dynamics

Fig. 3 illustrates the water absorption and the average pore size of specimens with MICP using DM obtained from the water absorption dynamics test. When the bacterial solution was used to replace 10% water, both the water absorption and the average pore size increased. When the replacement level reached 30%, both the water absorption and the average pore size dropped slightly, followed by a significant rise when the replacement level was 50%. It suggests that the replacement of 30% water with bacteria solution was beneficial to the drop in water absorption, as the addition of bacterial solution in SSC mortar reduced its pH value at initial, resulting in the formation of less early hydration product (i.e., ettringite) and increased the pore size. Low alkaline environment is beneficial to the survival of bacteria. With the process of bacterial metabolism, the in-situ deposition of bio calcium carbonate would fill in the pores and reduce the porosity, which shown the same phenomenon found in the research that the presence of $CaCO_3$ crystals could clog the pore[36]. On the other hand, with the gradual dissolution of GGBS, some $[SiO_4]$ or $[AlO_4]$ released and the reduced pH value of pore solution could improve the aggregation of $[SiO_4]$ or $[AlO_4]$ [37], promoting the hydration process and rising the content of C-S-H and C-A-H. The chemical reaction above could benefit to the formation of hydration products indirectly which further fill in the pores. When the substitution of water with bacteria solution reached 30%, under these combined actions, the water absorption and the average pore size were the lowest. However, the high alkaline environment would affect the survival of bacteria and the effects of the in-situ deposition bio calcium carbonate by bacterial metabolism and the increasing pH value would reduce, leading to the rise in water absorption and average pore size.

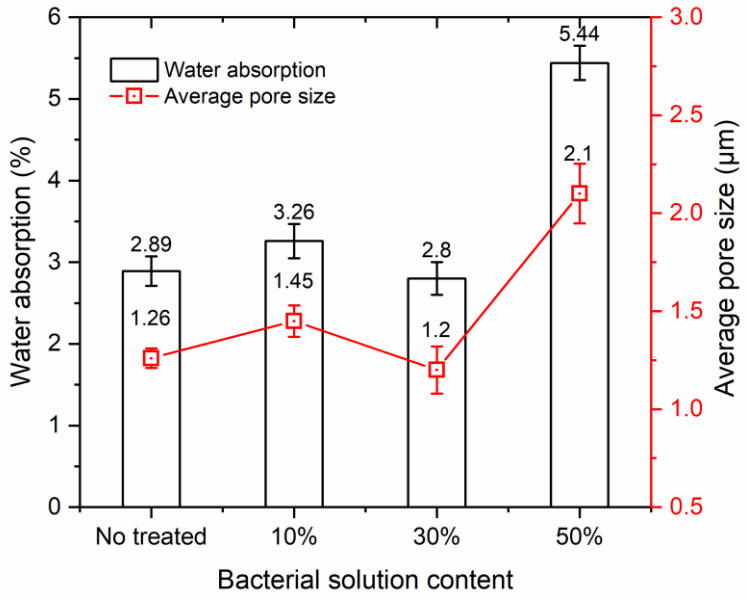

Fig. 3. Water absorption and average pore size of specimens with various bacterial solution contents.

3.2. Hydration products

As there is less influence of surface treatment with MICP on the phases of hydration products of sample's interior substance [30], only the mineral composition of the reference sample's interior substance was tested to evaluate the phase change of the surface layer and the matrix. Fig. 4 displays the mineral compositions of SSC mortars with treatment of MICP. For all samples, the diffraction peak intensity of silica was extremely high, which indicated that the content of silica was the highest, where the silica mainly came from the silica sand in mortar. Therefore, the influence of silica would be ignored on the change of hydration products. As seen in Fig. 4(a), the main hydration products of SSC mortars treated with TM are calcite and ettringite. We take the diffraction peak intensity of ettringite at about 16° and that of calcite at about 29° represent the contents of ettringite and calcite respectively. For the reference sample T-0, the diffraction peak of ettringite of the surface layer decreased slightly compared to the interior substance, about 5%, while that of calcite of the surface layer increased about 50% relative to the interior substance. The rising content of calcite might come from the carbonation reaction between ettringite and atmospheric CO_2, which was decomposed into calcium carbonate, gypsum, alumina gels and water, described as [19, 31, 38]:

$$3CaO \cdot Al_2O_3 \cdot 3CaSO_4 \cdot 32H_2O + 3H_2CO_3 \rightarrow 3CaCO_3 + 3CaSO_4 + Al_2O_3 \cdot XH_2O + (35 - X)H_2O \quad (4)$$

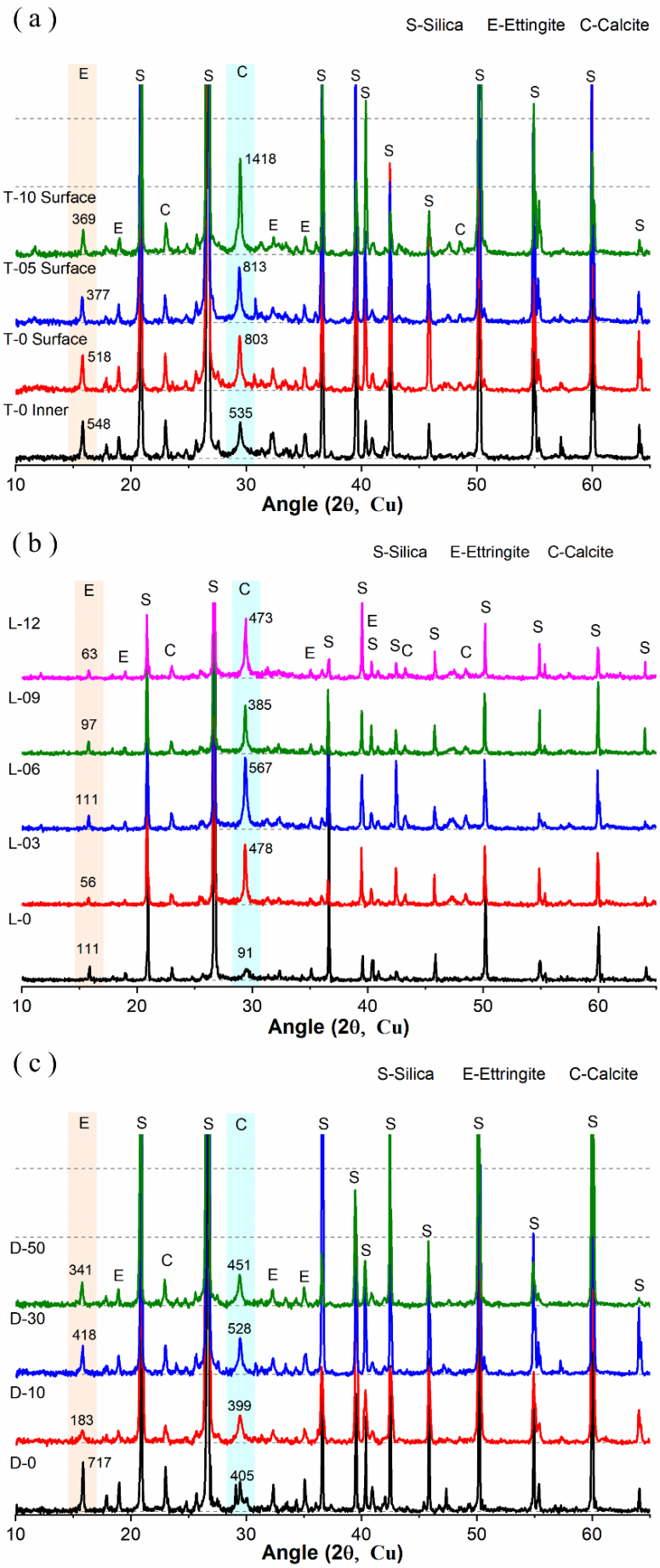

Fig. 4. Mineral compositions of specimens treated with (a) TM, (b) LM and (c) DM.

After surface treatment with TM, the diffraction peak of ettringite reduced gradually (about 27% and 29%) and that of calcite increased (about 1% and 77%) with the increase of B:S ratio from 0 to 1:1. The rise in the diffraction peak of calcite can be ascribed to the precipitation reaction of MICP on the surface layer. The precipitation content was higher when the B:S ratio was 1:1, leading to a more obvious diffraction peak of calcite and a high decrease rate. The slight decrease of ettringite can be associated with the influence of bacterial solution, which reduced the pH value of pore solution and promoted the decomposition of ettringite, which was transformed into AFm or other forms of calcium aluminate hydrate [37]. As seen in Fig. 4(b), the main hydration products of the surface layer of SSC mortars treated with LM were also calcite and ettringite. After surface treatment with LM, the diffraction peak intensity of calcite increased significantly, about from 3.2 to 5.2 times of the reference sample L-0, while that of ettringite decreased about from 0 to 50% compared to sample L-0. With the increase of treatment numbers, there is no obvious regularity of the change in the diffraction peak intensity of calcite and ettringite. Fig. 4(c) presents the main hydration products of SSC mortars with the increase of the proportion of bacterial solution to water. The main hydration products were silica, ettringite and calcite. The diffraction peak of calcite can also be found in the reference sample D-0 as it can be easy to be carbonated [4, 21, 39, 40]. The diffraction peak of ettringite was the highest. After the addition of bacterial solution in SSC mortar, the diffraction peak of calcite increased slightly, while that of ettringite reduced significantly. When the replacement level of bacterial solution to water was 30%, the diffraction peaks of calcite and ettringite were the highest among the treated samples, with calcite increment of 30% and ettringite reduction of 42%. When the replacement level was 10%, the diffraction peak of ettringite was the weakest with the reduction of 74%.

The above results imply that the diffraction peak of ettringite all reduced after treatment with MICP, while method with DM did get the highest reduction rate, and LM method got the lowest. The increase degree of the diffraction peak of calcite of specimens from the highest to the lowest are LM, TM and DM, which caused by the different dosage of MICP, that LM method with sufficient content of bacterial solution and cementation solution got the highest content of deposited calcite.

The TG-DTG curves of all SSC mortars are shown in Fig. 5. In general, for OPC, there are three decomposition peaks (also known as weight loss peaks, corresponding to the TG curves at the same temperature) at different temperature ranges in DTG curves, including that (i) before 200 °C, representing the loss of free and crystalline water of hydration products, such as gypsum, ettringite, C-S-H gel, (ii) from 400 to 500 °C, denoting the decomposition of portlandite, and (iii) from 500 to 700 °C, standing for the decomposition of calcite. While there are only two obvious decomposition peaks in DTG curves for SSC mortars: one happened before 200 °C and the other occurred between 500 and 700 °C. As seen in XRD test results (Fig. 4), the main hydration crystal products are ettringite and calcite, while C-S-H gel is another main hydration product in hardened SSC mortar [39, 41].

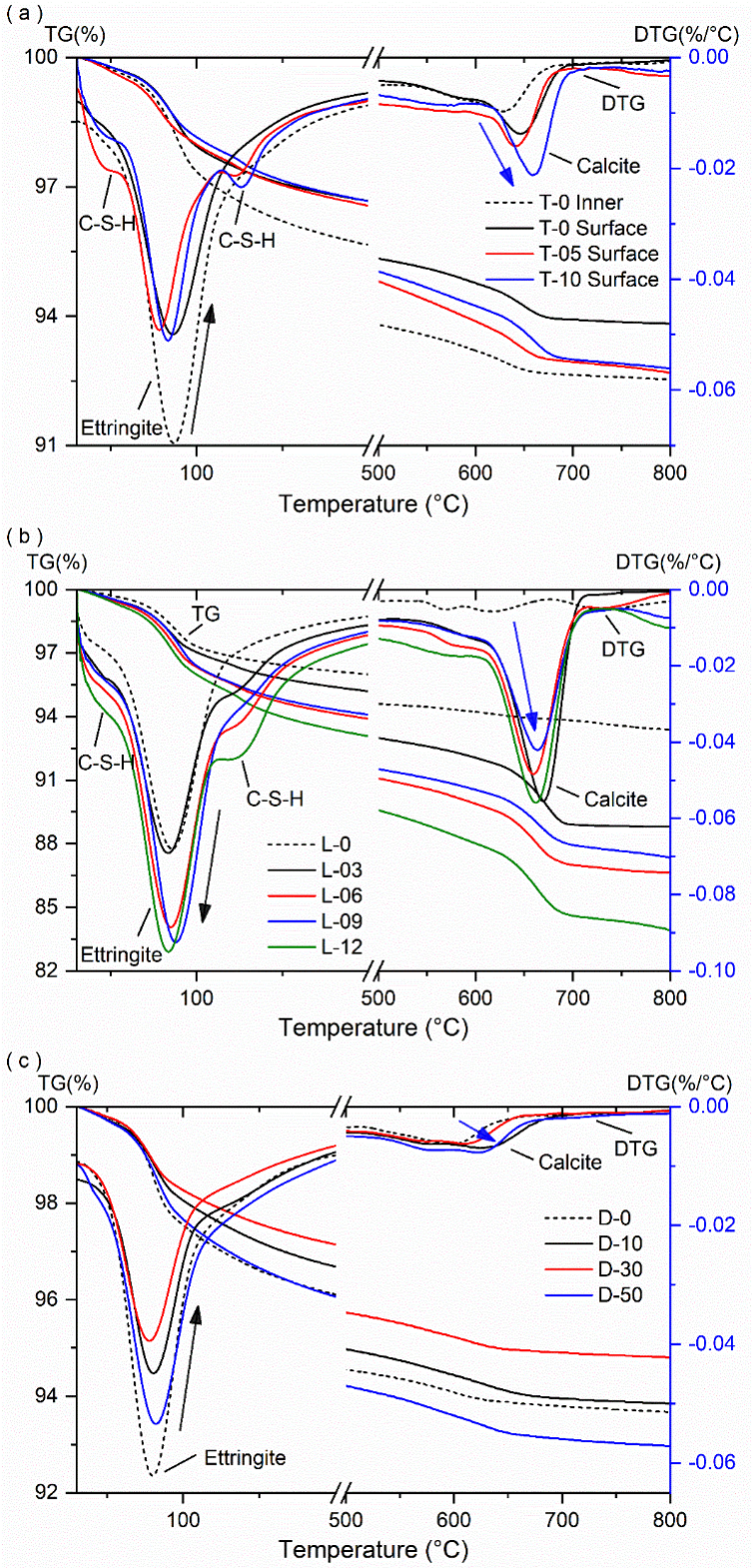

Fig. 5 TG-DTG curves of SSC mortars with treatment of (a) TM, (b) LM and (c) DM.

For specimens of TM in Fig. 5(a), the decomposition peak before 200 °C of the matrix was higher than other samples, and its decomposition peak at 500-700 °C was the lowest. Due to the carbonation of the surface in the air, the decomposition peak of calcite was higher than that of the matrix, and the surface treatment on surface made the gap even wider. The decomposition peak of calcite of sample T-5 with B:S = 1:2 increased slightly, while the decomposition peak of calcite of

sample T-10 with B:S = 1:1 was the highest, which are consistent with the XRD results. For LM specimens, as illustrated in Fig. 5(b), the reference sample L-0 exhibited the lowest decomposition peaks no matter before 200 °C or between 500 and 700 °C. The decomposition peaks before 200 °C and between 500 and 700 °C increased significantly after surface treatment with LM. The decomposition peak of calcite increased gradually with the increase of treatment cycles, while the increment was small. Therefore, increasing the treatment cycles did not lead to a significant increase in the content of calcite. As seen in Fig. 5(c), the reference sample D-0 had the highest decomposition peak before 200 °C and the lowest decomposition peak between 500 and 700 °C. After the addition of bacterial solution, the content of hydration products, especially ettringite, reduced obviously and calcite content increased slightly.

Fig. 6 demonstrates the weight loss of all samples at different temperature ranges calculated from TG-DTG curves. For specimens treated with TM, the weight loss before 200 °C of the reference sample's surface was lower than that of the inner substance due to the water evaporation of the surface. For the surface layer, after surface treatment the weight loss before 200 °C increased slightly, while the weight loss between 500 and 700 °C went up obviously. As for LM, the weight loss before 200 °C increased significantly after surface treatment but went up gradually with the increase of treatment cycles. The reason is that the tested surface was immersed in the liquid all the time and the water permeation could promote the hydration of the sample near the surface. The weight loss at 500-700 °C increased significantly after surface treatment but changed little with the increase of treatment cycles. More treatment cycles had less effect on the increase of calcite and 3 treatment cycles resulted in a significant rise in the content of calcite. As for DM, the weight loss before 200 °C dropped slightly and the weight loss at 500-700 °C increased slightly with the addition of bacterial solution. Compared to the methods of TM and LM, less calcite was formed for DM, implying that the DM method is detrimental to the formation of bio calcite. Put bacterial solution on the surface or add it in matrix directly would reduce the quantity of total hydration products (Fig. 6), especially for the content of ettringite (Fig. 4 and Fig. 5). Due to the low alkalinity of bacterial solution, which could reduce the alkalinity of pore solution and make ettringite unstable.

The results above indicated that the diffraction peak of ettringite decreased slightly and that of calcite increased significantly after surface treatment. The decreasing ettringite was caused by the influence of bacterial solution, which could reduce the alkalinity of the surface layer's pore solution and made ettringite unstable [42]. The obvious increasing calcite content can be mainly ascribed to the precipitation of calcite on the surface layer by MICP. When the B:S ratio was 1:1, the diffraction peak of calcite was stronger, while the diffraction peak of calcite changed little with the increase of treatment cycles. The calcite content of near surface layer played an important role in pore structure. The reaction products consisting of ettringite, C-S-H and calcite could fill in the pores and refine the

pore structure.

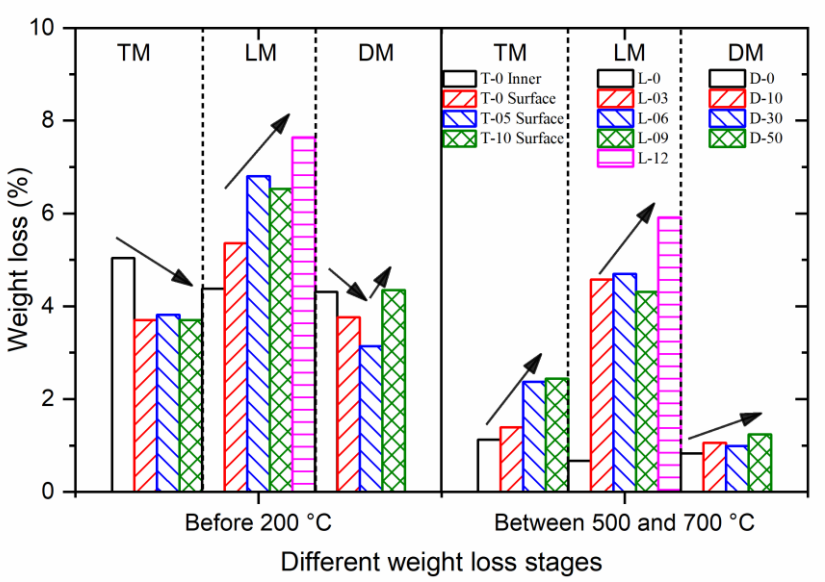

Fig. 6. Weight loss of SSC mortars at two temperature ranges.

3.3 Microstucture

3.3.1 Evolution of pore structure

Fig. 7 presents the pore size distribution including cumulative distribution and differential distribution of pore volume of SSC mortars with different treatment methods. For specimens with TM, the total pore volume reduced significantly after surface treatment, and the differential distribution curves shifted left, especially the volume of the pore size smaller than 0.01 μm that went up. For specimens with LM, after surface treatment the total pore volume reduced with the increase of treatment number, while the differential distribution changed in disorder. For specimens with DM, the effect of the addition of bacterial solution in SSC mortar on the drop in total pore volume was worse, and it was detrimental to the refine of pore structure. The differential distribution curves exhibited disorder rules with the increase of the proportion of bacterial solution replaced of water.

Based on the data shown in Fig. 7, the pore volume distribution and pore volume fraction distribution of SSC mortars can be calculated, which are summarised in Fig. 8. For specimens with TM, the total pore volume of the samples after surface treatment decreased with the increase of B:S ratio. The volumes of harmless pores and less harmful pores (<50 nm) [43] of samples T-05 and T-10 were about 0.022 and 0.025 mL/g, lower than that of the reference sample T-0 of 0.032 mL/g. While the volume fraction of pores with size small than 50 nm of sample T-10 increased, which was beneficial to the property of samples. It was indicated that specimens with surface treatment could lead to the change in pore volume distribution and refined the pore structure. For specimens with LM, the total pore volume of the samples after surface treatment dropped first with the increase of treatment numbers. When the treatment number was 9 times, the total pore volume of sample L-09 was the lowest. Although the total pore volume of specimens with LM decreased obviously, the

change of pore volume fraction was little, especially the volume fraction of pores with size <50 nm and only that of specimens L-03 and L-09 went up, which could refine the pore structure. For specimens with DM, the total pore volume of the samples after the addition of bacterial solution increased to some extent, while only that of sample D-30 reduced slightly. With the increase of replacement level of bacterial solution to water, pores with size <50 nm exhibited a rise in volume, especially the harmless pores (<20 nm) whose volume increased significantly and was the highest.

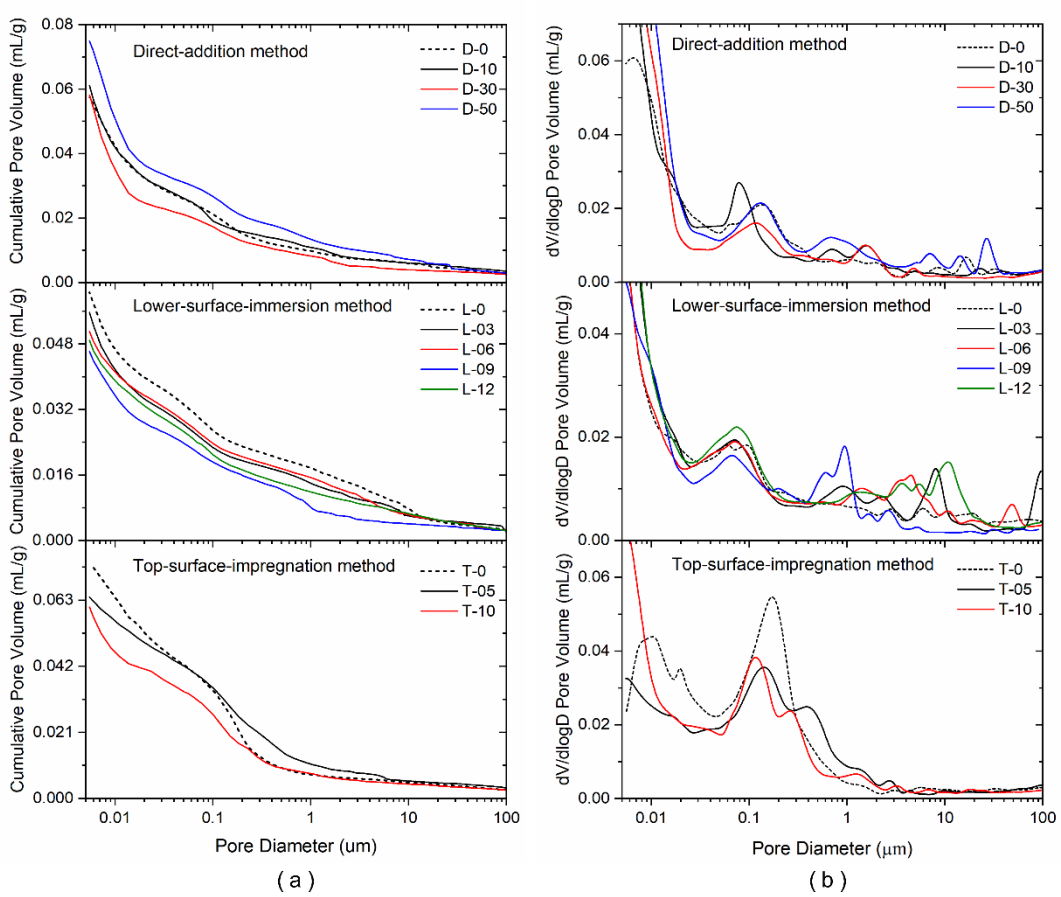

Fig. 7. Pore size distribution of SSC mortar under different treatment methods: (a) cumulative distribution of pore volume; (b) differential distribution of pore volume.

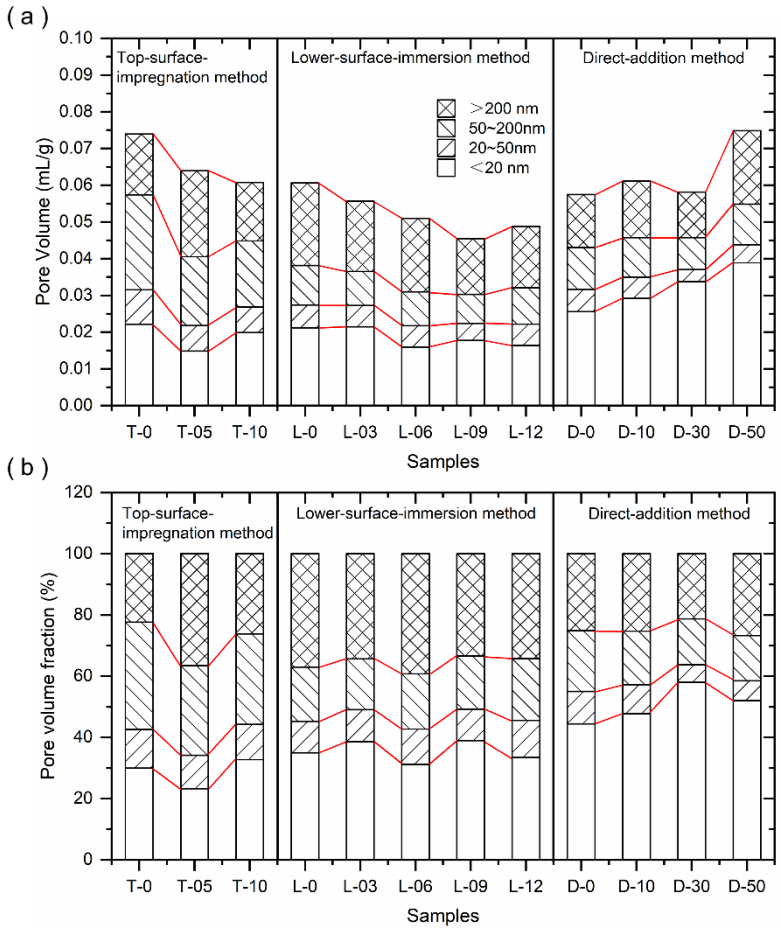

Fig. 8. (a) Pore volume and (b) pore volume fraction of SSC mortars.

3.3.2 Morphology

Fig. 9 illustrates the morphology of SSC mortar with surface treatment of TM. As seen in Fig. 9(a), the short bars and net substance C-S-H gels are found all over the fracture surface, and some pores are also can be observed obviously of the reference matrix T-0. Fig. 9(b) shows the surface morphology of the reference sample T-0, the surface is smooth relatively, some holes can be found on the surface and lots of needle materials formed in the holes. After surface treatment with TM, the surface was covered by spherical and square substances with different sizes, the size of the square substance is bigger than that of spherical substance (in Fig. 9(c) and (d)).

Fig. 10 shows the surface morphology of SSC mortar with the surface treatment of LM. As seen in Fig. 10(a) for the reference sample L-0, some small particle substances were on the surface and some holes with different sizes can also be found. For the surface morphology of specimen L-3 after surface treatment, as displayed in Fig. 10(b), the original surface was not so visible, while lots of irregular shaped substances appeared on the surface. After 6 times of treatment (Fig. 10(c)), the surface was covered with the precipitated substance all over, and the grain boundaries were barely discernible, where the surface of the precipitated particles was composed of densely packed small particles of material. After 9 and 12 times of surface treatment, besides the dense particles on the surface, there are some micro and nano spherical bio calcite produced, evenly scattered.

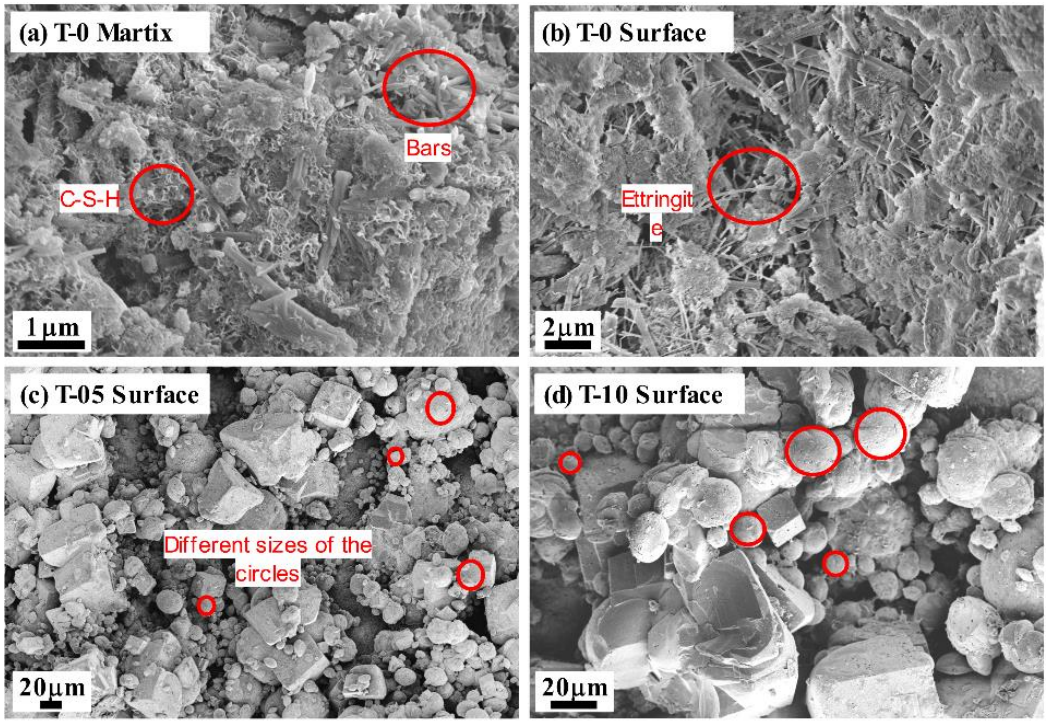

Fig. 9. Morphology of SSC mortars treated with TM.

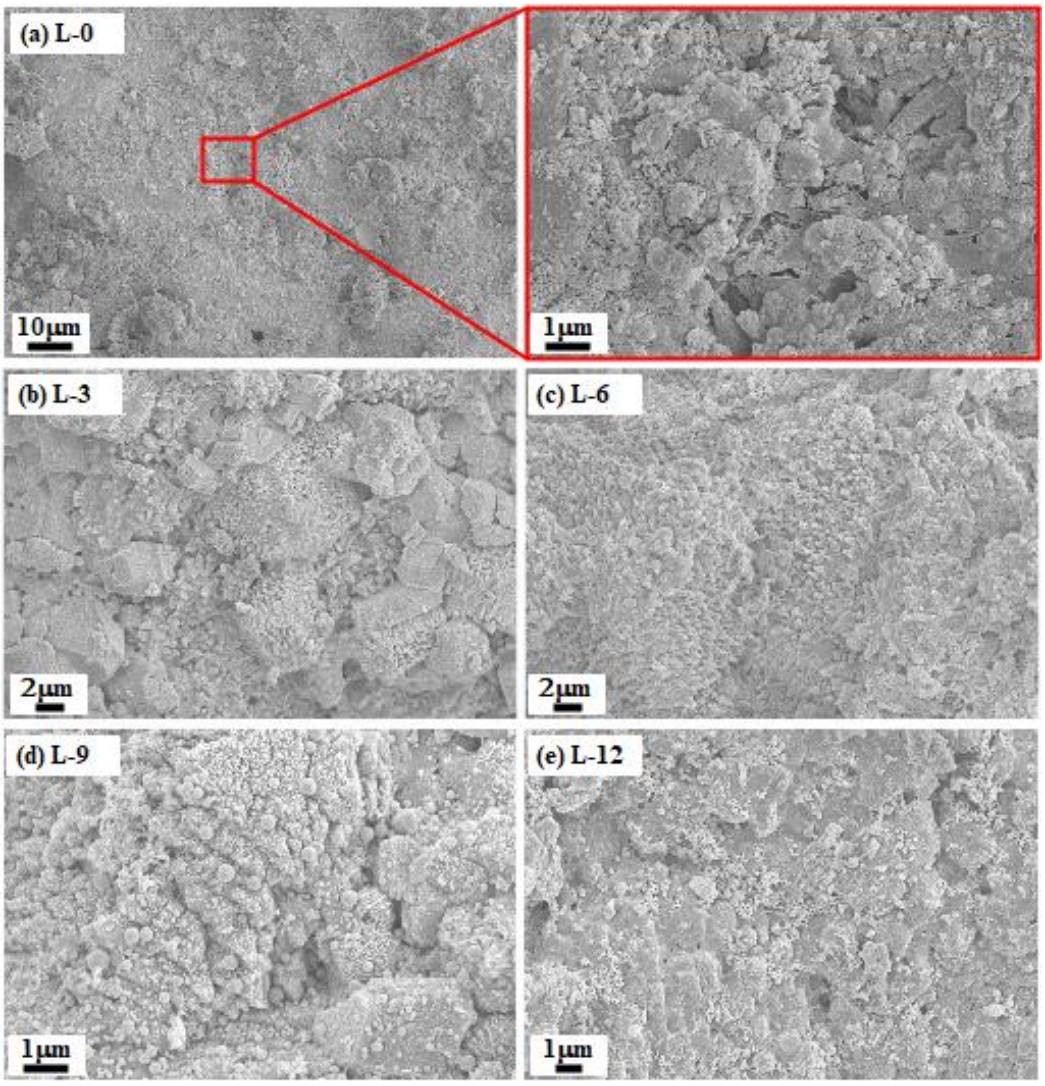

Fig. 10. Surface morphology SSC mortars treated with LM.

Fig. 11 illustrates the morphology of SSC mortar with MICP using DM. As seen in Fig. 11(a), the typical microstructure of SSC with different hydration products can be observed for the reference specimen D-0, where lots of needle bar granular ettringite. With the addition of bacterial solution, the content of needle bar granular ettringite reduced gradually. When the bacterial solution was used to replace 10% or 30% water, short bars can be found in Fig. 11(b) and (c). As the replacement level was increased to 50%, lots of near special substances can be observed, implying that with the increase of replacement level of water with bacteria solution, the shapes of hydration products changed from short bars to near spherical. With the decrease of alkalinity, the forming conditions of ettringite become progressively worse, resulting in the formation of coarse rods instead of regular needles [42]. Due to the different low alkalinity, the ettringite was unstable [31], and the change of volume happened, which could result in some cracks in the matrix. Although there are a small amount newly formed hydration products and bio calcite, it is not enough to fill the pores to achieve the desired effect. Therefore, DM method is not effective in improving the pore structure of matrix, and thus other better methods should be sought.

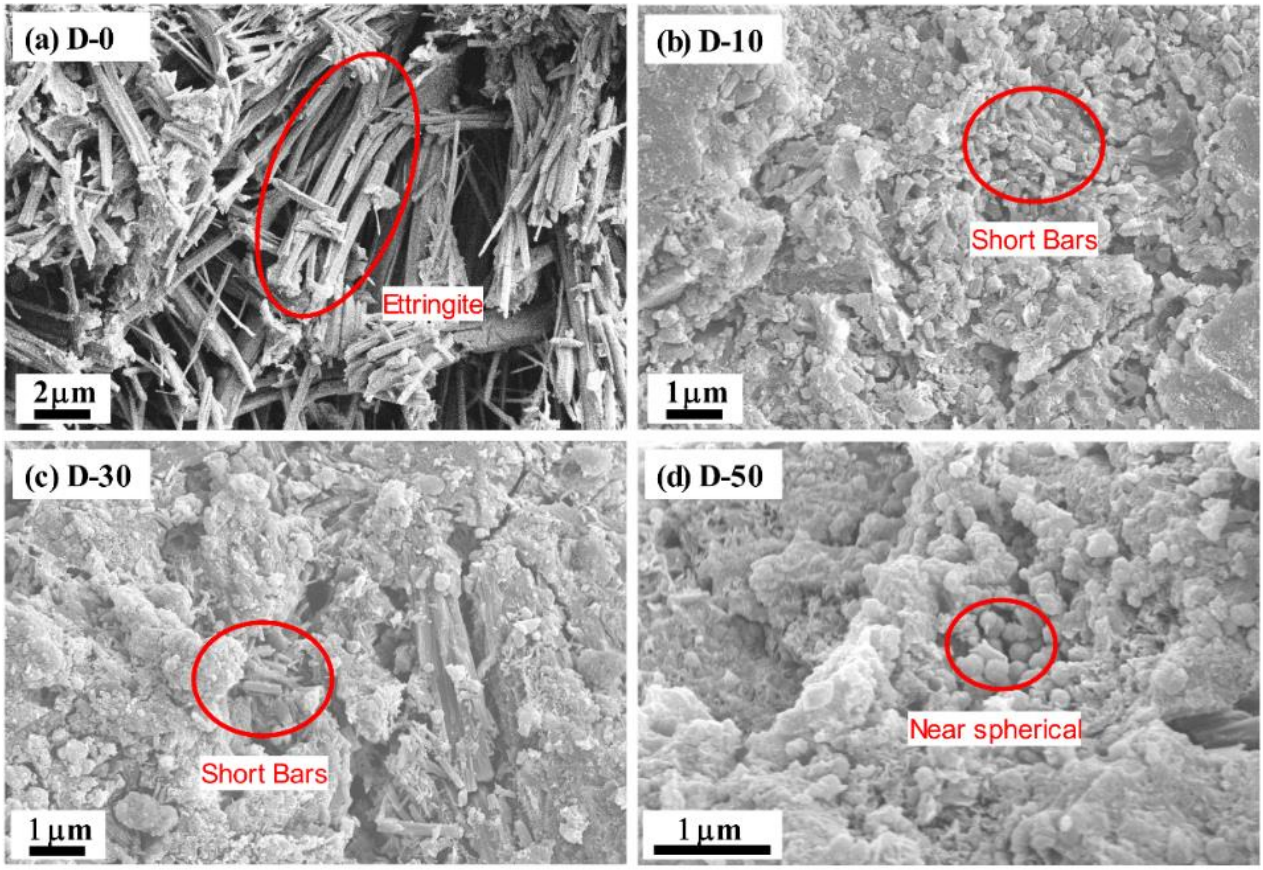

Fig. 11. Morphology of SSC mortars treated with DM.

4. Discussion

4.1. Effect of bacterial solution to cementation solution ratio

With the increase of B:S ratio, the absorption coefficient reduced slightly (Fig. 2), the quantity of formed bio calcite increased slightly (Fig. 6) and the diffraction peak of calcite increased

significantly (Fig. 4), while the total pore volume decreased. Compared to the reference specimens, when the B:S ratio was 1:2, the volume fraction of less harmful pore and harmless pore reduced and the porosity increased when B:S = 1:1, indicating a more obvious effect on porosity of less harmful and harmless pores than total porosity. The increase of pore volume fraction of less harmful pore and harmless pore is beneficial to the reduced water absorption. Regarding porosity, the volume fraction of pore size (<50 nm) of specimen T-10 increased significantly, especially for the harmless pores (<20 nm), which would make the interior pores smaller and thus is beneficial to pore structure [44, 45]. The capillary water absorption coefficient could be effectively reduced by optimising the surface structure and producing a deposition layer on the surface. Although the content of calcite increased slightly of B:S ratio from 1:2 to 1:1 (Fig. 6), the diffraction peak intensity of calcite increased significantly (Fig. 4), which implied that the crystallinity of calcite was improved when the bacterial solution proportion was elevated. Meanwhile high crystallinity calcite was more stable, which was conductive to pore filling. Research has pointed out that increase the content of bacterial solution appropriately is good for the yield and crystallinity of calcite [46]. Otherwise, the stability of high crystallinity calcite is better, which is beneficial to the effective filling of pores [47]. All these indicate that with the increase of B:S ratio, the content of bio calcite increased slightly, and the crystallinity of calcite was improved more, which could fill in the holes on surface and the pores near the surface to refine the pore structure of SSC mortar's surface layer.

4.2. Effect of treatment numbers

With the increase of treatment numbers, the absorption coefficient reduced gradually first and then increased slightly as the treatment number increased from 9 to 12 times (Fig. 2). The quantity of bio calcite increased significantly after surface treatment with LM and the change of calcite quantity among the treated samples is small, especially for specimen L-12 with an obvious rise (Fig. 6). The diffraction peak intensity of calcite changed little with the rising treatment numbers (Fig. 4). The total porosity reduced first with the increase of treatment numbers. When the treatment number was 9 times, the total pore volume of sample L-09 was the lowest. The formed bio calcite on the surface filled some pores of the surface layer and led to the reduced water absorption coefficient.

At early stage of treatment, the drop in absorption coefficient can be attributed to the further hydration of SSC with the permeation of water through capillary pores. When the lower surface was immersed in bacterial solution, some bacteria can be absorbed and thus the in-situ precipitation of bio calcite was formed on the surface layer, leading to the reduction of absorption coefficient. Meanwhile, the bacterial metabolism could increase the pH value, facilitating the further hydration of SSC, and thus more hydration products were formed, filling in the pores and reducing the coefficient. When the sample was immersed in the cementation solution, the absorbed bacteria on the surface can interact with enough urea and calcium ions to precipitate more bio calcium carbonate. Otherwise, the

permeation of bacterial solution into the surface layer could reduce the alkalinity of pore solution and induce decomposition of some ettringite to enlarge the surface pores. Accordingly, the low alkalinity has a great influence on the surface pores due to the sufficient bacterial solution under surface treatment with LM. As a result, enough bacterial solution and cementation solution could precipitate more bio calcite, which is much more than that of specimens with TM and DM. With the increase of treatment numbers, the quantity and diffraction peak intensity of calcite among the treated specimens changed little. The drop in total porosity resulted in the reduction of water absorption coefficient.

4.3. Effect of bacterial solution content

The addition of bacterial solution in SSC mortar reduced the diffraction peak intensity of ettringite significantly and increased the diffraction peak intensity of calcite slightly (Fig. 4). With the increase of bacterial solution content, the water absorption and average pore size increased, expect for sample D-30. The pH value of the stable bacterial solution was about 9.5 [33]. The pH value of pore solution in SSC mortar was lower than in ordinary Portland cement mortar but still higher than that of bacterial solution. When the bacterial solution was added to replace of water, it would reduce the alkalinity of SSC mortar at the early hydration period and hinder the formation of ettringite. However, the formation of ettringite was slow and hydration products were formed with the dissolution of the system as well as some ettringite. When the proportion of bacteria solution was 30% or 50%, the reduction of ettringite diffraction peak was small. The possible reason is that more microorganisms are conducive to the stability of ettringite, which offsets the adverse effect on ettringite due to reduced alkalinity. The addition of bacterial solution increased the intensity of calcite's diffraction peak slightly, induced by the action of MICP, which happened in pores of SSC mortars. Although the alkaline of SSC was low, which was beneficial to the survival of bacteria, the addition of bacterial solution directly cannot increase the content of calcite obviously.

Although the total porosity of SSC mortars went up with the increasing addition of bacterial solution, the volume fractions of less harmful pore and harmless pore also increased. Especially for sample D-30, the volume fractions of less harmful pore and harmless pore were the highest and accordingly its water absorption coefficient was the smallest. Thus, the effect of volume fractions of less harmful pore and harmless pore (pore size < 50 nm) on water absorption is more significant than that of total porosity.

4.4. Effect of treatment method

The capillary water absorption coefficient of SSC mortar reduced to some extent after surface treatments with TM and LM, depending on the filling effect of the precipitated bio calcite on the surface layer. When the total volume of bacterial solution and cementation solution are fixed, the key factor for the absorption coefficient reduction effect is the property of bio calcite, such as quantity, shape and size of bio calcite, and the change of pore structure could be another form to reveal the

effect.

The average reduction in water absorption coefficient of specimens with TM was higher than that of specimens with LM (Fig. 2), while the intensity of diffraction peak of bio calcite of specimens with TM was higher than that of specimens with LM (Fig. 4), especially for specimen T-10, indicating a higher crystallinity of bio calcite of specimen with TM. The shapes of bio calcite of specimen with TM were spherical and square (Fig. 9), with most size at micro level, which can fill the pores of the surface effectively, while the morphology of precipitated layer of specimen with LM (Fig. 10) had no fixed shapes, which may be covered on the surface. From the size and shape of bio calcite points of view, the surface treatment with TM had a better effect on water absorption coefficient than surface treatment with LM. However, the quantity of formed bio calcite is also important. As indicated in the TGA results (Fig. 6), the quantity of formed bio calcite of specimens with LM was much higher than that of specimens with TM. As specimens with LM had sufficient bacterial solution and cementation solution for precipitation during the surface treatment, more bio calcite was formed, while it had its less effect on the coefficient reduction than specimens with TM, which can be ascribed to the drop in pH value when the bacterial solution was permeating into the surface of SSC mortar and the shape and crystallinity of bio calcite were worse compared to that of specimens with LM.

The average water absorption of specimens with DM was higher than that of reference specimen D-0, which indicated a less significant effect on the reduced water absorption in comparison with those treaded with TM and LM. After treatment of DM, the alkalinity of pore solution in SSC mortar reduced significantly, hindering the formation of ettringite and leading to large pores of the matrix. Although the low alkalinity is beneficial to the survival of bacteria that can absorb the calcium ions and generate bio calcium carbonate to fill pores, the quantity of bio calcite was limit, much less than those of surface treatment with TM and LM (Fig. 4 and Fig**. 6**). Calcium ions needed for MICP come from four aspects, pore solution, decomposition of ettringite, decalcification of C-S-H gels and cementation solution. Due to the insufficient cementation solution, the formed bio calcite was few and more calcium ions from the decomposition of ettringite and decalcification of C-S-H gels would react with carbanion from MICP. As a result, the content of ettringite and C-S-H gels would reduce, and their morphologies and space structures would change. Thus, the enhancement effect of DM in SSC mortar was smallest. It was indicated that after surface treatment, some harmful pores could transform to harmless pores, reducing the pore size and refining the pore structure [27, 48]. As a result, TM had a most significant effect on the water absorption coefficient of SSC mortar, followed by LM and DM, while MICP surprisingly led to a rise in volume of harmless pores (<20 nm).

Surface treatment with TM and LM exhibited a more obvious effect on the decrease of total porosity of SSC mortar, compared to DM. Surface treatment can reduce the total porosity directly as the calcium carbonate sediment was formed on the surface, which can fill in the surface pores and

improve the pore structure. In addition, during the surface treatment, some bacterial solution and cementation solution might permeate into samples and generate some calcium carbonate to fill or clog the inner pores, thus refining the pore structure. For DM, there was no obvious precipitation lay on the surface, while some calcium carbonate was also precipitated in the pores of the whole sample and its effect on the reduction of total porosity was small. The addition of bacterial solution in SSC mortars increased the total pore volume obviously, especially for sample D-50, the total pore volume of which was the highest, as well as the water absorption coefficient (Fig. 3).

The results indicated that the reductions of the water absorption coefficient of SSC specimens with TM and LM were obvious, suggesting that the surface modification effect of surface treatment with MICP is superior to the addition of bacterial solution directly. A higher drop in water absorption coefficient can be observed for specimens with TM, in comparison with that with LM, implying a more effectiveness of TM on the modification of the surface than LM.

5. Conclusions

To improve the property of SSC mortar, top-surface-impregnation method (TM) and lower-surface-immersion method (LM) focusing on surface property, and direct-addition method (DM) focusing on the whole property were employed to evaluate their effects on water absorption property, hydration products and the microstructure of the surface and the internal fracture surface, aiming to find an effective method for enhanced surface property of SSC mortar. Based on the experimental results obtained, the main conclusions can be drawn as follows:

(1) The effect of surface treatment with TM and LM on the reduction of water absorption is superior to that of DM, and TM is superior to LM. Calcium carbonate deposition layer was formed on the surface directly under the surface treatment, which can reduce the water absorption of the surface obviously. However, a small amount of calcium carbonate was formed inside the matrix, which had a limited effect on reducing the water absorption.

(2) The surface treatment method with proper condition could optimise the pore structure of the surface layer, reduce the total porosity, and increase the volume fractions of harmless and less harmful pores, especially harmless pores, which is beneficial to improve the surface property of SSC mortar. A certain content of bio calcite can reduce the absorption and porosity, while the morphology and size of bio calcite play important roles when at high content.

(3) After surface treatment, the content of ettringite dropped slightly but the calcite content went up significantly. The content of calcite increased the most when the B:S ratio was 1:1 under TM. The increase of treatment number had a limited effect on the increase of calcite content, while could refine the pore structure and reduce the absorption coefficient when the treatment cycle was 9 times. DM had a great influence on the alkalinity of SSC mortar, which could significantly reduce the content of ettringite and slightly increase the calcite content.

(4) After surface treatment, the surface of SSC mortar was covered by a layer of calcium carbonate deposition, presenting spherical or square particles, which can fill the surface holes. DM changed the morphology of ettringite in matrix from needle rod to short rod or even spherical, resulting in internal microcracks but it had a slight effect on pore filling.

From the conclusions above, proper treatment methods with MICP technology can enhance the surface property of SSC. Then the widespread application of SSC can be improved, which will reduce the use of traditional cement and increase the utilization rate of phosphogypsum.

Declaration of competing interest

The authors declare that they have no known competing financial interests or personal relationships that could have appeared to influence the work reported in this paper.

Acknowledgements

The authors greatly acknowledge the financial support from the National Key R&D Program of China (2022YFC3801605), the National Natural Science Foundation of China (52278273), the CRSRI Open Research Program (Program SN：CKWV20221026/KY), and the Key Research and Development Program of Hubei Province (2022BCA059).

References

[1] M.C.G. Juenger, F. Winnefeld, J.L. Provis, J.H. Ideker, Advances in alternative cementitious binders, Cement and Concrete Research. 41(2011)1232-1243, https://doi.org/10.1016/j.cemconres.2010.11.012.

[2] J.S. Damtoft, J. Lukasik, D. Herfort, D. Sorrentino, E.M. Gartner, Sustainable development and climate change initiatives, Cement and Concrete Research. 38(2008)115-127, https://doi.org/10.1016/j.cemconres.2007.09.008.

[3] P. Hajek, Concrete structures for sustainability in a changing world, Procedia Engineering. 171(2017)207-214, https://doi.org/10.1016/j.proeng.2017.01.328.

[4] Z. Sun, S. Nie, J. Zhou, H. Li, Z. Chen, M. Xu, R. Mu, Y. Wang, Hydration mechanism of calcium sulfoaluminate-activated supersulfated cement, Journal of Cleaner Production. 333(2022) https://doi.org/10.1016/j.jclepro.2021.130094.

[5] S.R. Pinto, C. Angulski da Luz, G.S. Munhoz, R.A. Medeiros-Junior, Resistance of phosphogypsum-based supersulfated cement to carbonation and chloride ingress, Construction and Building Materials. 263(2020) https://doi.org/10.1016/j.conbuildmat.2020.120640.

[6] J. Neeraj, G. Mridul, Formulation of sulphate resistant super sulphated cement using fluorogypsum and granulated blast furnace slag, IOSR Journal of Mechanical and Civil Engineering. 12(2015)153-159, https://doi.org/10.9790/1684-1232153159.

[7] S. Liu, L. Wang, B. Yu, Effect of modified phosphogypsum on the hydration properties of the phosphogypsum-based supersulfated cement, Construction and Building Materials. 214(2019)9-16, https://doi.org/10.1016/j.conbuildmat.2019.04.052.

[8] S. Liu, L. Wang, Y. Gao, B. Yu, Y. Bai, Comparing study on hydration properties of various cementitious systems, Journal of Thermal Analysis and Calorimetry. 118(2014)1483-1492, https://doi.org/10.1007/s10973-014-4052-4.

[9] K. Cabrera-Luna, E.E. Maldonado-Bandala, D. Nieves-Mendoza, P. Castro-Borges, J.I.E. García, Novel low emissions supersulfated cements of pumice in concrete; mechanical and electrochemical characterization, Journal of Cleaner Production. 272(2020)122520, https://doi.org/10.1016/j.jclepro.2020.122520.

[10] Y. Zhou, Z. Peng, L. Chen, D. Xu, H. Wang, Double-sided tuning effects of lactic acid on the

hydration, microstructure and strength of supersulfated cement, Journal of Sustainable Cement-Based Materials. 2022)1-14, https://doi.org/10.1080/21650373.2022.2027829.
[11] M.B. Haha, B. Lothenbach, G. Le Saout, F. Winnefeld, Influence of slag chemistry on the hydration of alkali-activated blast-furnace slag - Part II: Effect of Al2O3, Cement and Concrete Research. 42(2012)74-83, https://doi.org/10.1016/j.cemconres.2011.08.005.
[12] M.B. Haha, B. Lothenbach, G. Le Saout, F. Winnefeld, Influence of slag chemistry on the hydration of alkali-activated blast-furnace slag - Part I: Effect of MgO, Cement and Concrete Research. 41(2011)955-963, https://doi.org/10.1016/j.cemconres.2011.05.002.
[13] M.M. Smadi;, R.H. Haddad;, A.M. Akour, Potential use of phosphogypsum in concrete, Cement and Concrete Research. 29(1999)1419-1425, https://doi.org/10.1016/S0008-8846(99)00107-6.
[14] K.J. Mun, W.K. Hyoung, C.W. Lee, S.Y. So, Y.S. Soh, Basic properties of non-sintering cement using phosphogypsum and waste lime as activator, Construction and Building Materials. 21(2007)1342-1350, https://doi.org/10.1016/j.conbuildmat.2005.12.022.
[15] S. Liu, P. Fang, J. Ren, S. Li, Application of lime neutralised phosphogypsum in supersulfated cement, Journal of Cleaner Production. 272(2020)122660, https://doi.org/10.1016/j.jclepro.2020.122660.
[16] J.S. Andrade Neto, J.D. Bersch, T.S.M. Silva, E.D. Rodríguez, S. Suzuki, A.P. Kirchheim, Influence of phosphogypsum purification with lime on the properties of cementitious matrices with and without plasticizer, Construction and Building Materials. 299(2021)123935, https://doi.org/10.1016/j.conbuildmat.2021.123935.
[17] A.R.D. Costa, S.R.C. Matos, G. Camarini, J.P. Gonçalves, Hydration of sustainable ternary cements containing phosphogypsum, Sustainable Materials and Technologies. 28(2021)e00280, https://doi.org/10.1016/j.susmat.2021.e00280.
[18] K. Gu, B. Chen, Y. Pan, Utilization of untreated-phosphogypsum as filling and binding material in preparing grouting materials, Construction and Building Materials. 265(2020)120749, https://doi.org/10.1016/j.conbuildmat.2020.120749.
[19] S. Liu, J. Ouyang, J. Ren, Mechanism of calcination modification of phosphogypsum and its effect on the hydration properties of phosphogypsum-based supersulfated cement, Construction and Building Materials. 243(2020)118226, https://doi.org/10.1016/j.conbuildmat.2020.118226.
[20] B. Gracioli, C. Angulski da Luz, C.S. Beutler, J.I. Pereira Filho, A. Frare, J.C. Rocha, M. Cheriaf, R.D. Hooton, Influence of the calcination temperature of phosphogypsum on the performance of supersulfated cements, Construction and Building Materials. 262(2020)119961, https://doi.org/10.1016/j.conbuildmat.2020.119961.
[21] S.R. Pinto, C. Angulski da Luz, G.S. Munhoz, R.A. Medeiros-Junior, Durability of phosphogypsum-based supersulfated cement mortar against external attack by sodium and magnesium sulfate, Cement and Concrete Research. 136(2020)106172, https://doi.org/10.1016/j.cemconres.2020.106172.
[22] R. Novak, W. Schneider, E. Lang, New knowledge regarding the supersulphated cement slagstar, ZKG International. 58(2005)70-78.
[23] H. Nguyen, T.P. Chang, J.Y. Shih, C.T. Chen, Formulating for innovative self-compacting concrete with low energy super-sulfated cement used for sustainability development, Journal of Materials Science and Chemical Engineering. 4(2016)22-28, https://doi.org/10.4236/msce.2016.47004.
[24] Q. Wu, Q. Xue, Z. Yu, Research status of super sulfate cement, Journal of Cleaner Production. 294(2021)126228, https://doi.org/10.1016/j.jclepro.2021.126228.
[25] W. De Muynck, K. Cox, N.D. Belie, W. Verstraete, Bacterial carbonate precipitation as an alternative surface treatment for concrete, Construction and Building Materials. 22(2008)875-885, https://doi.org/10.1016/j.conbuildmat.2006.12.011.
[26] W. De Muynck, D. Debrouwer, N. De Belie, W. Verstraete, Bacterial carbonate precipitation improves the durability of cementitious materials, Cement and Concrete Research. 38(2008)1005-1014, https://doi.org/10.1016/j.cemconres.2008.03.005.
[27] Q. Chunxiang, W. Jianyun, W. Ruixing, C. Liang, Corrosion protection of cement-based building

materials by surface deposition of CaCO3 by Bacillus pasteurii, Materials Science and Engineering: C. 29(2009)1273-1280, https://doi.org/10.1016/j.msec.2008.10.025.
[28] J. Xu, W. Yao, Z.W. Jiang, Non-ureolytic bacterial carbonate precipitation as a surface treatment strategy on cementitious materials, Journal of Materials in Civil Engineering. 26(2014)983-991, https://doi.org/10.1061/(ASCE)MT.
[29] J. Xu, X.Z. Wang, W. Yao, Coupled effects of carbonation and bio-deposition in concrete surface treatment, Cement & Concrete Composites. 104(2019)103358, https://doi.org/10.1016/j.cemconcomp.2019.103358.
[30] L. Wang, Z. Ren, H. Wang, X. Liang, S. Liu, J. Ren, Y. He, M. Zhang, Microstructure-property relationships in cement mortar with surface treatment of microbial induced carbonate precipitation, Composites Part B: Engineering. 239(2022)109986, https://doi.org/10.1016/j.compositesb.2022.109986.
[31] Y. Xie, T. Sun, Z. Shui, C. Ding, W. Li, The impact of carbonation at different CO2 concentrations on the microstructure of phosphogypsum-based supersulfated cement paste, Construction and Building Materials. 340(2022)127823, https://doi.org/10.1016/j.conbuildmat.2022.127823.
[32] J. Xu, X. Wang, Self-healing of concrete cracks by use of bacteria-containing low alkali cementitious material, Construction and Building Materials 167 (2018) 1-14, https://doi.org/10.1016/j.conbuildmat.2018.02.020.
[33] L. Wang, S. Liu, J. Ren, Effect of low-temperature treatment on bacterial cultivation in bacterial induced mineralization, Science China Technological Sciences. 65(2021)870-881, https://doi.org/10.1007/s11431-021-1937-5.
[34] L. Wang, S. Liu, Mechanism of sand cementation with an efficient method of microbial-induced calcite precipitation, Materials. 14(2021)5631, https://doi.org/10.3390/ma14195631.
[35] Wang RX, Qian CX, Wang JY, Cheng L. Different treated methods of microbiologically deposited CaCO3 layer on hardened cement paste surface. J Chin Ceram Soc 2008;36:1378-84, DOI:10.14062/j.issn.0454-5648.2008.10.021.
[36] S. Joshi, S. Goyal, M.S. Reddy, Influence of nutrient components of media on structural properties of concrete during biocementation, Construction And Building Materials 158 (2018) 601-613, https://doi.org/10.1016/j.conbuildmat.2017.10.055.
[37] X.J. Zhang, G.Z. Zhang, D.S. Sun, Effect of pH-value of Na2SO4 solution on the structure of C-(A)-S-H gels in Portland cement pastes, Acta Materiae Compositae Sinica. 36(2019)441-449, https://doi.org/10.13801/j.cnki.fhclxb.20180427.001.
[38] C. Xiantuo, Z. Ruizhen, C. Xiaorong, Kinetic study of ettringite carbonation reaction, Cement and Concrete Research 24(7) (1994) 1383-1389, https://doi.org/10.1016/0008-8846(94)90123-6.
[39] S. Rubert, C.A.D. Luz, M.V.F. Varela, J.I. Pereira Filho, R.D. Hooton, Hydration mechanisms of supersulfated cement: The role of alkali activator and calcium sulfate content, Journal of Thermal Analysis and Calorimetry. 134(2018)971-980, https://doi.org/10.1007/s10973-018-7243-6.
[40] F. Puertas, B. González-Fonteboa, I. González-Taboada, M.M. Alonso, M. Torres-Carrasco, G. Rojo, F. Martínez-Abella, Alkali-activated slag concrete: Fresh and hardened behaviour, Cement and Concrete Composites. 85(2018)22-31, https://doi.org/10.1016/j.cemconcomp.2017.10.003.
[41] Q. Dong, Mechanical Properties of Modified Supersulfated Cement Mortar, Ceramics - Silikaty. 2021)255-262, https://doi.org/10.13168/cs.2021.0026.
[42] P.O. Trentin, M. Perardt, R.A. Medeiros-Junior, Ettringite instability analysis in the hydration process of the supersulfated cement, Journal of Thermal Analysis and Calorimetry. 147(2021)6631-6642, https://doi.org/10.1007/s10973-021-11005-9.
[43] Z.W. Wu, H.Z. Lian, High performance concrete. 1999, Beijing: China Railway Pubilshing House.
[44] T. Hoang, N.T. Dung, C. Unluer, J. Chu, Use of microbial carbonation process to enable self-carbonation of reactive MgO cement mixes, Cement and Concrete Research. 142(2021)106391,

https://doi.org/10.1016/j.cemconres.2021.106391.
[45] V. Whiffn, Microbial CaCO3 Precipitation for the production of biocement. 2004, Perth, Australia: Murdoch University.
[46] D. Sarda, H.S. Choonia, D.D. Sarode, S.S. Lele, Biocalcification by Bacillus pasteurii urease: a novel application, J Ind Microbiol Biotechnol 36(8) (2009) 1111-5, https://www.ncbi.nlm.nih.gov/pubmed/19415357.
[47] S.S. Bang, J.J. Lippert, U. Yerra, S. Mulukutla, V. Ramakrishnan, Microbial calcite, a bio-based smart nanomaterial in concrete remediation, International Journal of Smart and Nano Materials 1(1) (2010) 28-39, https://doi.org/10.1080/19475411003593451.
[48] V. Achal, Characterization of two urease-producing and calcifying bacillus spp. Isolated from cement, Journal of Microbiology and Biotechnology. 20(2010)1571-1576, https://doi.org/10.4014/jmb.1006.06032.